Nationaal Lucht- en Ruimtevaartlaboratorium
National Aerospace Laboratory NLR

NLR-TP-2001-369

Brittle archaeological silver: a fracture mechanisms assessment

R.J.H. Wanhill

Nationaal Lucht- en Ruimtevaartlaboratorium
National Aerospace Laboratory NLR

NLR-TP-2001-369

Brittle archaeological silver : a fracture mechanisms assessment

R.J.H. Wanhill

This report has been prepared as a contribution to the archaeometallurgical literature.

Division: Structures and Materials
Issued: 14 August 2001
Classification of title: Unclassified

Contents

BRITTLE ARCHAEOLOGICAL SILVER : A FRACTURE MECHANISMS ASSESSMENT

R.J.H. Wanhill
National Aerospace Laboratory NLR, Anthony Fokkerweg 2,
1059 CM Amsterdam, The Netherlands

ABSTRACT

Archaeological silver may be embrittled by long-term corrosion and microstructural changes. The embrittlement increases with increasing grain size, and the combination of a large grain size with synergistic embrittlement (conjoint action of corrosion-induced and microstructurally-induced embrittlement) is particularly detrimental. Micromechanical models of cracking that incorporate the grain size provide insight into the severity of embrittlement. Severely embrittled artifacts are frangible or even friable.

KEYWORDS: ARCHAEOLOGICAL SILVER, EMBRITTLEMENT, GRAIN SIZE, CRACKS, FRACTURE.

INTRODUCTION

Archaeological silver may be brittle owing to long-term corrosion and microstructural changes (Thompson and Chatterjee 1954; Werner 1965; Ravich 1993; Wanhill *et al*. 1998; Wanhill 2000, 2001a). Corrosion-induced embrittlement and microstructurally-induced embrittlement may be independent of each other but can also act synergistically (Wanhill *et al*. 1998; Wanhill 2000, 2001a).

Metallographic observations have shown that the grain size is an important factor for archaeological silver embrittlement. Large-grained artifacts appeared to be more susceptible to cracking (Werner 1965). Also, the combination of a large grain size with synergistic embrittlement is particularly detrimental (Wanhill *et al*. 1998).

The present work assesses these observations using micromechanical models of cracking. To do this it is necessary first to describe the types of embrittlement and the concept of grain boundary character. However, the physical and chemical mechanisms of embrittlement are discussed

elsewhere, as are the diagnostic techniques and remedial measures (Wanhill *et al*. 1998; Wanhill 2000, 2001a).

TYPES OF EMBRITTLEMENT

Corrosion-induced embrittlement

Archaeological silver undergoes general corrosion, which results in a brittle, finely granular surface layer of silver chloride (Gowland 1918; Scott 1996; Wanhill 2000, 2001a). This surface corrosion does not affect the remaining metal's integrity, although unfavourable conditions may result in an artifact being completely converted to silver chloride (Gowland 1918).

Even so, some artifacts experience localised corrosion that penetrates the silver and enables embrittlement due to cracking along the corrosion paths (Werner 1965; Ravich 1993; Wanhill *et al.* 1998). Examples are shown in figure 1. Intergranular corrosion can occur in mechanically worked and annealed artifacts. Interdendritic corrosion can occur in castings with essentially as-cast microstructures, i.e. little changed by any subsequent mechanical working or annealing, see Scott (1996). Corrosion along slip lines and deformation twin boundaries can occur in an artifact that has not been annealed after final mechanical working, which includes chased and stamped decorations (Wanhill *et al.* 1998): inside the silver these forms of corrosion can lead to additional corrosion along segregation bands. These bands are the remains, modified by mechanical working and annealing heat-treatments, of solute element segregation (coring) and interdendritic segregation that occurred during solidification of an ingot or cupelled button.

Cracking along the corrosion paths in the silver usually results in irregular fracture surfaces with a finely granular appearance. However, highly localised corrosion along slip lines and deformation twin boundaries results in crystallographic fractures, for example the fractograph in figure 1.

Microstructurally-induced embrittlement

This type of embrittlement is most probably a consequence of long-term low temperature ageing, whereby segregation of an impurity element, or elements, occurs to grain boundaries (Wanhill *et al.* 1998; Wanhill 2000, 2001a). Cracking appears to be entirely intergranular, and examples are shown in figure 2. The cracks are characteristically narrow and sharp (unlike intergranular corrosion, see figure 1) except where grains can become bodily displaced, which is itself a characteristic of severe embrittlement. One such displacement is shown in the SEM fractograph of figure 2.

The grain boundary fracture facets are initially clean. Long-term environmental exposure can cause the facets to become locally corroded where slip lines, deformation twin boundaries and segregation bands intersect the fracture surfaces.

Synergistic embrittlement

As stated in the introduction, corrosion-induced and microstructurally-induced embrittlement can act synergistically (Wanhill *et al.* 1998; Wanhill 2000, 2001a). Figure 3 gives examples of the appearances of synergistic embrittlement. Corrosion along slip lines, deformation twin boundaries and segregation bands can result in cracks under the action of external loads or forces (e.g. crushing pressures during interment) and internal residual stresses due to retained cold-work. These cracks can then initiate fracture along microstructurally embrittled grain boundaries – which may fracture anyway, though less easily – under the action of external loads or forces. In turn, grain boundary fractures expose more slip lines, deformation twins and segregation bands to the environment and therefore increase the opportunities for corrosion.

GRAIN BOUNDARY CHARACTER

Grain boundaries strongly influence the properties of metals and alloys. This was first recognised in the derivation of "laws" describing property-dependence on a length scale, usually the average grain size or diameter, d. Examples are the Herring-Nabarro relationship for the strain rate in creep controlled by lattice diffusion of vacancies, $\dot{\varepsilon} \propto d^{-2}$; the Coble relationship for the strain rate in creep controlled by grain boundary diffusion of vacancies, $\dot{\varepsilon} \propto d^{-3}$; and the Hall-Petch relationships for plastic yield stress, $\sigma_y \propto d^{-1/2}$, or fracture stress, $\sigma_f \propto d^{-1/2}$ (Herring 1950; Nabarro 1948; Coble 1963; Hall 1951; Petch 1953).

These length scale criteria assume all grain boundaries are similar. However, there is now much evidence that grain boundaries have different properties depending on their character, i.e. their type and structure (Chadwick and Smith 1976; Baluffi 1980; Watanabe 1984, 1993, 1994; Watanabe *et al.* 1980, 1989; Lim and Watanabe 1990).

From the literature and their own research Watanabe (1984, 1993, 1994) and Watanabe *et al.* (1980, 1989) suggested dividing grain boundaries into three character- and property-determined categories: low-angle boundaries with misorientation angles less than 15°, high-angle

coincidence boundaries with low Σ* coincidence, and high-angle random boundaries. The basic distinguishing feature is that low-angle and low Σ coincidence boundaries are low-energy boundaries, while random boundaries are high-energy boundaries.

This distinction between grain boundary types and structures is relevant to microstructurally-induced embrittlement of archaeological silver, for two reasons:

(1) Most silver artifacts were made using combinations of mechanical working and annealing heat-treatments. The resulting microstructures will have mainly high-angle random grain boundaries, see by analogy Watanabe (1984) and Watanabe *et al.* (1989). This means the artifacts will contain many grain boundaries susceptible to microstructurally-induced embrittlement, assuming that impurity element segregation has occurred (Wanhill 2001a).

(2) A preponderance of high-angle random grain boundaries makes it reasonable, and indeed compatible with empirical observations (Werner 1965), to consider embrittlement in terms of length scale criteria based on the average grain size or diameter, d.

EMBRITTLEMENT FRACTURE MECHANISMS

Microcrack initiation

Embrittlement is manifested by cracking under the action of external loads or forces and internal residual stresses, if present. Cracking begins with *microcracks* smaller than or equal to the grain size. At this size or length scale the average grain size or diameter, d, symbolising a preponderance of high-angle random grain boundaries, is likely to strongly influence crack initiation.

Figure 4 depicts microcrack models applicable to archaeological silver embrittlement. A full discussion of these models, in mainly non-mathematical detail, is given in Wanhill (2001b). The following sub-paragraphs summarise the models.

- Figure 4a: This is the classic dislocation pile-up model of microcrack initiation, applicable to corrosion-induced and microstructurally-induced embrittlement, whereby corrosion or

* A coincidence boundary is a lattice plane in both contiguous grains. A boundary with *low* Σ coincidence means the contiguous grains have orientations resulting in a *high* density of coincident lattice sites on the boundary.

impurity element segregation reduce the grain boundary fracture energy. The criterion for initiation of a grain boundary microcrack is obtained from Smith and Barnby (1967):

$$\tau_{app} - \tau_i \geq \sqrt{\frac{2\pi\mu\gamma_f}{(1-\nu)\,d}} \bullet \frac{1}{\sqrt{F(\theta)}} \qquad (1)$$

where τ_{app} = applied shear stress; τ_i = lattice friction stress; μ = shear modulus; γ_f = grain boundary fracture energy; ν = Poisson's ratio; d = grain diameter; $F(\theta)$ = an angular function; S = dislocation source; $\perp$, $\upharpoonleft$ = edge dislocations of opposite sign.

- Figures 4b-4d: These models are applicable to corrosion-induced and synergistic embrittlement, whereby microcracks develop due to corrosion along slip planes and facilitate initiation of microcracks at grain boundaries weakened by corrosion or impurity element segregation. The criteria for initiation of grain boundary microcracks are:

Fig. 4b 2a < d	$\tau_{app} \geq \sqrt{\frac{2\pi\mu\gamma_f}{(1-\nu)\,d}} \bullet \frac{1}{\left(1 - \frac{2\tau_i}{\pi\tau_{app}} \bullet \cos^{-1}\left(\frac{a}{d/2}\right)\right)} \bullet \frac{1}{\sqrt{F(\theta)}}$	(2)
Fig. 4c 2a = d	$\tau_{app} \geq \sqrt{\frac{2\pi\mu\gamma_f}{(1-\nu)\,d}} \bullet \frac{1}{\sqrt{F(\theta)}}$	(3)
Fig. 4b 2a = d multiple slip plane cracks	$\tau_{app} \geq \sqrt{\frac{2\pi\mu\gamma_f}{(1-\nu)\,d}} \bullet \frac{1}{\left(\sqrt{\frac{3h}{\pi d}} \bullet \left(\frac{d}{h} + 0.2865\right)\right)} \bullet \frac{1}{\sqrt{F(\theta)}}$	(4)

where h is the distance between multiple slip plane cracks (see, for example, figure 3). Equations (2) - (4) are derived from equation (1) and the analyses of Tanaka *et al*. (1986) for equation (2) and Tada *et al*. (1973) for equation (4). N.B. For mathematical simplicity these models assume the material to be elastically isotropic and homogeneous. On the scale of individual grains this is incorrect for most metals, including silver (Smithells 1967), but this does not invalidate a generic assessment.

The models make the general prediction that the applied shear stress, τ_{app}, required for initiation of a grain boundary microcrack decreases with increasing grain size, d, and decreasing grain

boundary fracture energy, γ_f. In fact, $\tau_{app} \propto d^{-1/2}$, which is the same as the Hall-Petch fracture stress relationship mentioned at the beginning of the section on grain boundary character. This effect of grain size on the stress required for grain boundary microcrack initiation is very significant. To illustrate this, figure 5 plots ratios of applied shear stress, $\tau_{app_2} / \tau_{app_1}$, versus ratios of average grain diameter, d_2/d_1, whereby it is assumed that small and large grain sizes in archaeological silver are represented by d_1 = 5-10 μm and d_2 = 100-200 μm, respectively. Figure 5 shows that the applied shear stress required for grain boundary microcrack initiation in the large-grained silver would be only 1/3 – 1/6 that for the fine-grained silver.

With respect to the grain boundary fracture energy, γ_f, a larger grain size can have two effects that promote grain boundary microcracking:

(1) *Intergranular corrosion*. A large grain size facilitates penetration of intergranular corrosion into an artifact. This is clearly demonstrated by Werner's metallograph in figure 1. The artifact concerned is a severely embrittled Roman cup (Werner 1965) with grain sizes up to 0.4 mm, which is nearly the full thickness.

(2) *Impurity element segregation*. Microstructurally-induced embrittlement caused by impurity element segregation to grain boundaries is likely to be exacerbated by a larger grain size. This will be explained using the schematics in figure 6, which show two possible dependences of the degree of embrittlement, represented by the local fracture stress, σ_f, on impurity element concentration at grain boundaries.
Figure 6a shows a "threshold" concept of embrittlement, for which the local fracture stress abruptly drops to a minimum value at a critical impurity concentration C_{cr}. This concept predicts no effect of grain size on embrittlement once C_{cr} is reached. Figure 6b shows a more realistic representation of embrittlement (Thompson and Knott 1993), whereby the local fracture stress decreases gradually to a minimum at a critical impurity concentration C^*_{cr}. For this behaviour larger grain sizes can increase embrittlement: larger grains mean less grain boundary area to be embrittled by the impurity elements in an artifact, and hence increased concentrations of impurities at the grain boundaries and increased embrittlement.

Microcracks to macrocracks: frangibility and friability

As discussed above, microcrack initiation along embrittled grain boundaries will be easier if the grain size is large. Furthermore, a preponderance of high-angle random grain boundaries means that archaeological silver artifacts will contain many grain boundaries susceptible to impurity element segregation and hence microstructurally-induced embrittlement, *if it has occurred*. The

combination of large grain size and a preponderance of high-angle random grain boundaries in a microstructurally embrittled artifact means many potential initiation sites for microcracks, and hence an increased possibility for microcracks to link up and become macrocracks. In other words, a large-grained microstructurally embrittled artifact is likely to be frangible, even if there is no damage from corrosion.

A severely corroded large-grained artifact *will* be frangible (Werner 1965). And the combination of a large grain size with synergistic embrittlement is even worse: corrosion increases the possibilities for microcrack initiation at microstructurally embrittled grain boundaries, as discussed with reference to figures 3 and 4, and the artifact can become friable (Wanhill *et al*. 1998).

CONCLUSIONS

(1) Embrittlement of archaeological silver may be considered in terms of length scale criteria based on the average grain size or diameter. Micromechanical models of cracking that incorporate the grain size provide insight into the severity of embrittlement.

(2) Larger grains increase embrittlement in several ways:
- by facilitating penetration of intergranular corrosion
- by enabling increased grain boundary concentrations of impurities causing microstructurally-induced embrittlement
- by facilitating grain boundary microcrack initiation, which may be involved in corrosion-induced, microstructurally-induced and synergistic embrittlement
- by providing many potential initiation sites for microcracks and hence an increased possibility for microcracks to become macrocracks.

(3) Severely embrittled artifacts are frangible or even friable.

REFERENCES

Baluffi, R.W. (ed.), 1980, Grain Boundary Structure and Kinetics, American Society for Metals (ASM), Metals Park, Ohio, U.S.A.

Chadwick, G.A., and Smith, D.A. (eds.), 1976, Grain Boundary Structure and Properties, Academic Press, London, U.K.

Coble, R.L., 1963, A model for boundary diffusion controlled creep in polycrystalline materials, Journal of Applied Physics, 34, 1679-1682.

Gowland, W., 1918, Silver in Roman and earlier times: I. Pre-historic and proto-historic times, Archaeologia, 69, 121-160.

Hall, E.O., 1951, The deformation and ageing of mild steel: III discussion of results, Proceedings of the Physical Society of London, B64, 747-753.

Herring, C., 1950, Diffusional viscosity of a polycrystalline solid, Journal of Applied Physics, 21, 437-445.

Lim, L.C., and Watanabe, T., 1990, Fracture toughness and brittle-ductile transition controlled by grain boundary character distribution (GBCD) in polycrystals, Acta Metallurgica et Materialia, 38, 2507-2516.

Nabarro, F.R.N., 1948, Deformation of crystals by the motion of single ions, Report of a Conference on the Strength of Solids, 75-90, The Physical Society, London, U.K.

Petch, N.J., 1953, The cleavage strength of polycrystals, Journal of the Iron and Steel Institute, 174, 25-28.

Ravich, I.G., 1993, Annealing of brittle archaeological silver: microstructural and technological study, in 10th Triennial Meeting of the International Council of Museums Committee for Conservation, Preprints of the Seminar: August 22/27, 1993, II, 792-795, Washington, D.C., U.S.A.

Scott, D.A., 1996, Technical study of a ceremonial Sican tumi figurine, Archaeometry, 38, 305-311.

Smith, E., and Barnby, J.T., 1967, Crack nucleation in crystalline solids, Metal Science Journal, 1, 56-64.

Smithells, C.J., 1967, Metals Reference Book, Volume 3, Fourth Edition, 708, 709, Butterworths, London, U.K.

Tada, H., Paris, P.C., and Irwin, G.R., 1973, The Stress Analysis of Cracks Handbook, 14.5, Del Research Corporation, St. Louis, Missouri, U.S.A.

Tanaka, K., Akiniwa, Y., Nakai, Y., and Wei, R.P., 1986, Modelling of small fatigue crack growth interacting with grain boundary, Engineering Fracture Mechanics, 24, 803-819.

Thompson, A.W., and Knott, J.F., 1993, Micromechanisms of brittle fracture, Metallurgical Transactions A, 24A, 523-534.

Thompson, F.C., and Chatterjee, A.K., 1954, The age-embrittlement of silver coins, Studies in Conservation, 1, 115-126.

Wanhill, R.J.H., Steijaert, J.P.H.M., Leenheer, R., and Koens, J.F.W., 1998, Damage assessment and preservation of an Egyptian silver vase (300-200 BC), Archaeometry, 40, 123-137: also NLR Technical Publication NLR TP 95372 L, National Aerospace Laboratory NLR, Amsterdam, The Netherlands.

Wanhill, R.J.H., 2000, Brittle archaeological silver. Identification, restoration and conservation, Materialen, 16, 30-35: also NLR Technical Publication NLR TP 97647 L, National Aerospace Laboratory NLR, Amsterdam, The Netherlands.

Wanhill, R.J.H., 2001a, Microstructurally-induced embrittlement of archaeological silver, NLR Technical Publication NLR-TP-2001-032, National Aerospace Laboratory NLR, Amsterdam, The Netherlands.

Wanhill, R.J.H., 2001b, The role of grain size in embrittlement of archaeological silver, NLR Technical Publication NLR-TP-2001-125, National Aerospace Laboratory NLR, Amsterdam, The Netherlands.

Watanabe, T., Kitamura, S., and Karashima, S., 1980, Grain boundary hardening and segregation in alpha iron-tin alloy, Acta Metallurgica, 28, 455-463.

Watanabe, T., 1984, An approach to grain boundary design of strong and ductile polycrystals, Res Mechanica, 11, 47-84.

Watanabe, T., Fujii, H., Oikawa, H., and Arai, K.I., 1989, Grain boundaries in rapidly solidified and annealed Fe-6.5 mass % Si polycrystalline ribbons with high ductility, Acta Metallurgica, 37, 941-952.

Watanabe, T., 1993, Grain boundary design and control for high temperature materials, Materials Science and Engineering, A166, 11-28.

Watanabe, T., 1994, The impact of grain boundary character distribution on fracture in polycrystals, Materials Science and Engineering, A176, 39-49.

Werner, A.E., 1965, Two problems in the conservation of antiquities: corroded lead and brittle silver, in Application of Science in Examination of Works of Art (Editor W.J. Young), 96-104, Boston Museum of Fine Arts, Boston, Massachusetts, U.S.A.

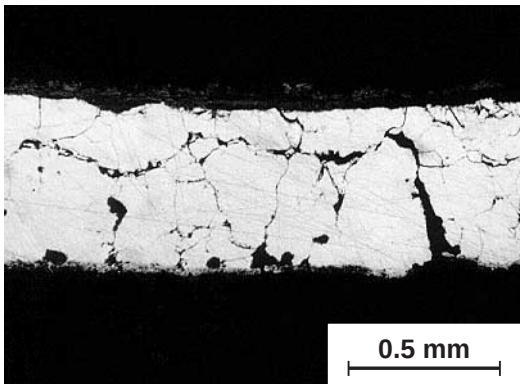

Intergranular corrosion: metallograph (Werner 1965)

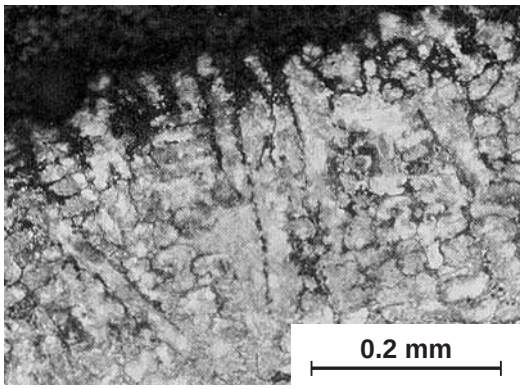

Interdendritic corrosion: metallograph (Scott 1996)

Slip line, deformation twin boundary and segregation band corrosion

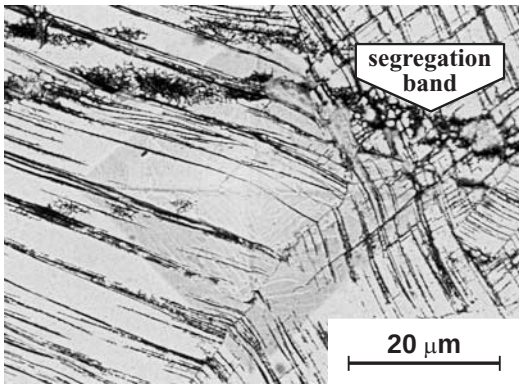

SEM metallograph (Wanhill *et al.* 1998)

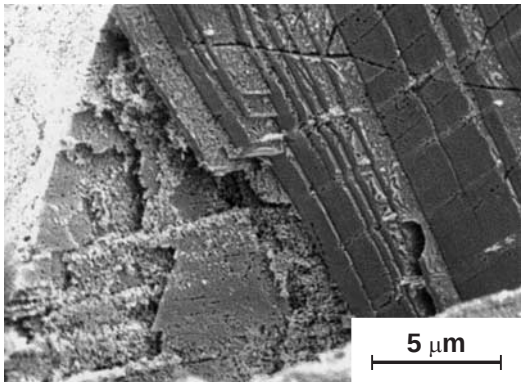

SEM fractograph (Wanhill *et al.* 1998)

Fig. 1 Examples of localised corrosion of archaeological silver:
SEM = Scanning Electron Microscopy

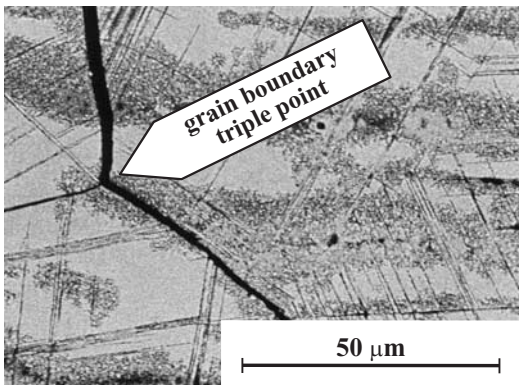

SEM metallograph (Wanhill *et al.* 1998)

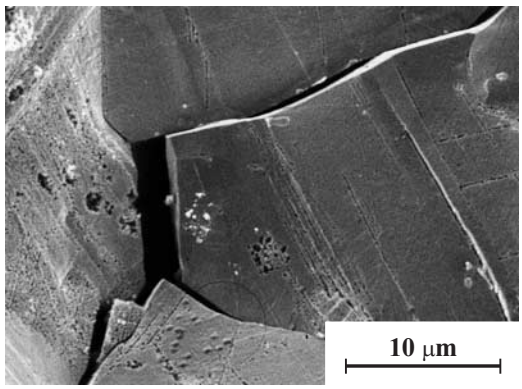

SEM fractograph (Wanhill *et al.* 1998)

Fig. 2 Microstructurally-induced intergranular fracture in archaeological silver:
SEM = Scanning Electron Microscopy

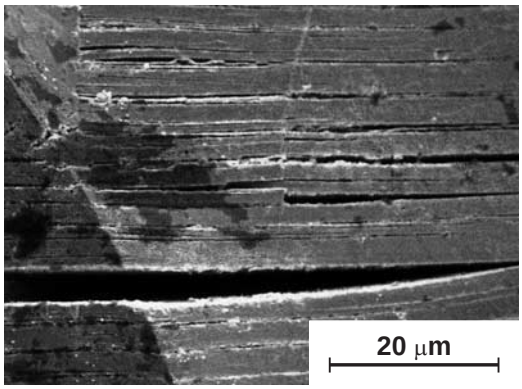

Corrosion along slip lines intersecting grain boundary facets: SEM fractograph (Wanhill *et al.* 1998)

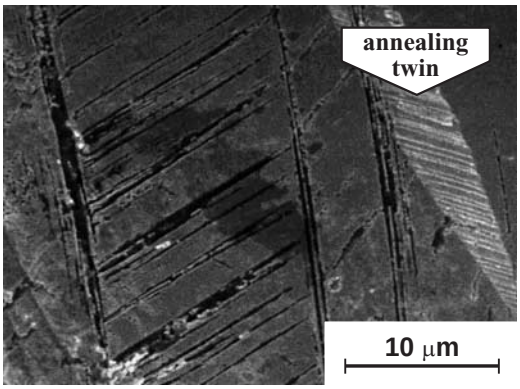

Corrosion along deformation twin boundaries intersecting a grain boundary facet: SEM fractograph (Wanhill *et al.* 1998)

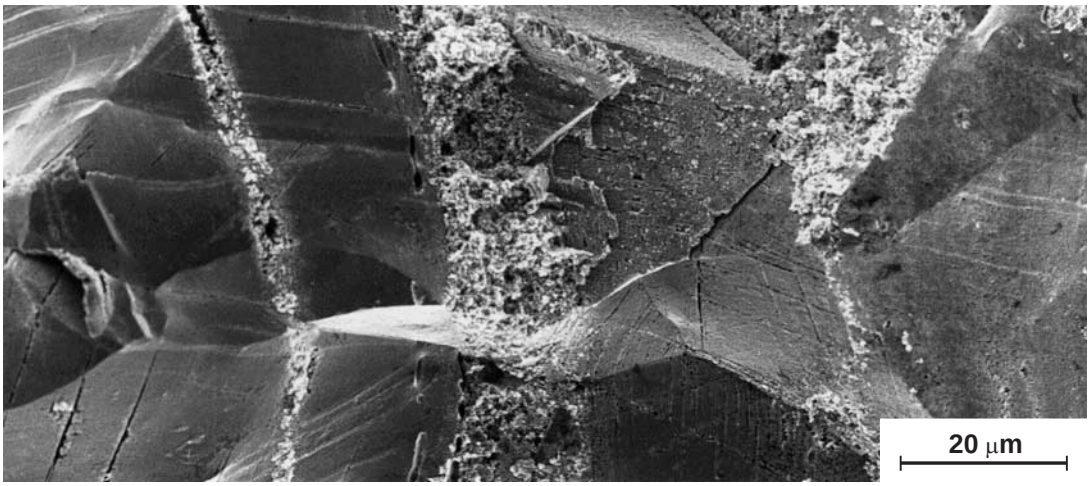

Corrosion along segregation bands intersecting grain boundary facets: SEM fractograph (Wanhill *et al.* 1998)

Fig. 3 Examples of synergistic embrittlement owing to microstructurally-induced embrittlement (intergranular fracture) and corrosion-induced embrittlement along slip lines, deformation twin boundaries and segregation bands: SEM = Scanning Electron Microscopy

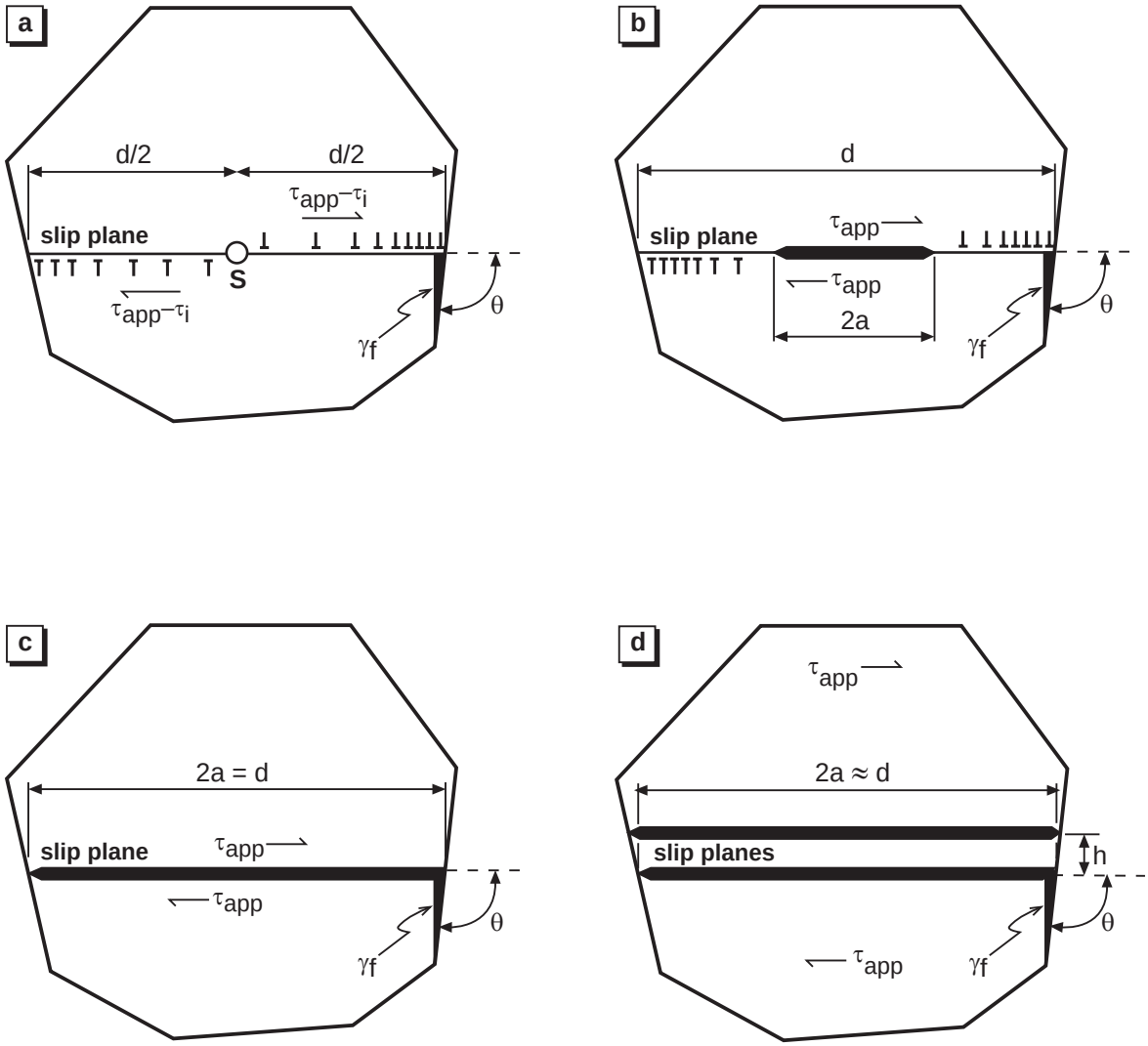

Fig. 4 Models of microcrack initiation at grain boundaries in embrittled archaeological silver. τ_{app} = applied shear stress; τ_i = lattice friction stress; γ_f = grain boundary fracture energy; 2a = slip plane crack length; d = grain diameter; h = distance between parallel slip plane cracks; S = dislocation source; ⊥, ⊤ = edge dislocations of opposite sign

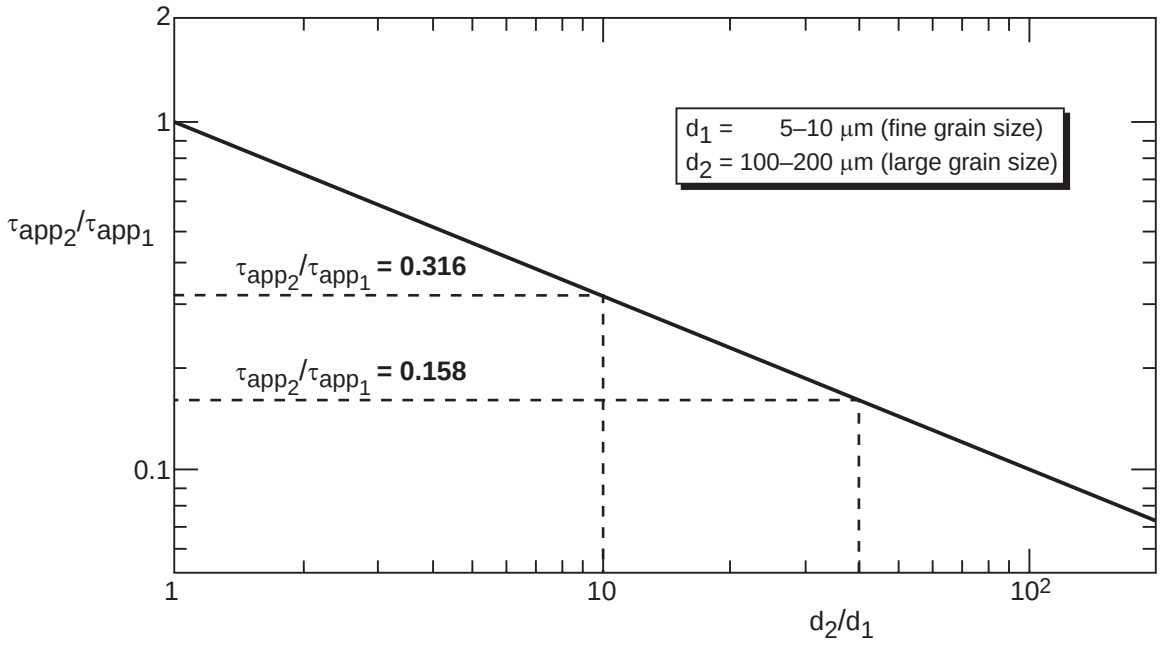

Fig. 5 Dimensionless plot of the applied shear stress, τ_{app}, versus average grain diameter, d, using the proportionality $\tau_{app} \propto \sqrt{1/d}$

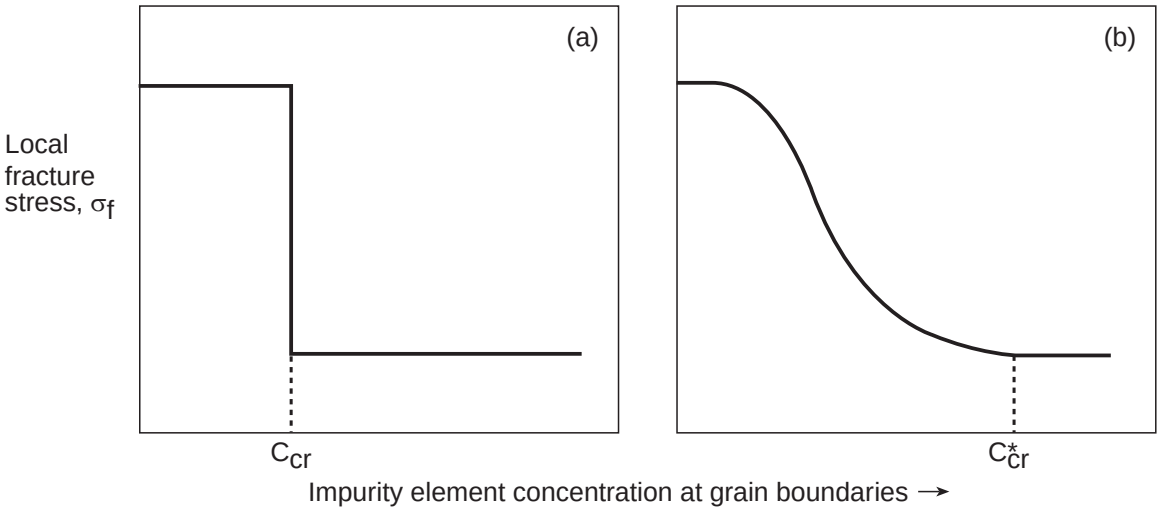

Fig. 6 Dependence of local fracture stress, σ_f, on impurity element concentration at grain boundaries: (a) "threshold" model behaviour in which fracture stress is abruptly lowered at a critical impurity element concentration, C_{cr}; (b) more realistic behaviour with fracture stress gradually decreasing to a minimum at a critical impurity element concentration, C^*_{cr}. After Thompson and Knott (1993)